Anti-inflammatory activity of IgG1 mediated by Fc galactosylation and association of FcγRIIB and dectin-1

Christian M Karsten[1,14], Manoj K Pandey[2,14], Julia Figge[1], Regina Kilchenstein[1], Philip R Taylor[3], Marcela Rosas[3], Jacqueline U McDonald[3], Selinda J Orr[3], Markus Berger[4], Dominique Petzold[4], Veroniqué Blanchard[4], André Winkler[5], Constanze Hess[5], Delyth M Reid[6], Irina V Majoul[7], Richard T Strait[8], Nathaniel L Harris[2], Gabriele Köhl[1], Eva Wex[9], Ralf Ludwig[10], Detlef Zillikens[10], Falk Nimmerjahn[11], Fred D Finkelman[2,12,13], Gordon D Brown[6], Marc Ehlers[1,5] & Jörg Köhl[1,2]

Complement is an ancient danger-sensing system that contributes to host defense, immune surveillance and homeostasis[1]. C5a and its G protein–coupled receptor mediate many of the proinflammatory properties of complement[2]. Despite the key role of C5a in allergic asthma[3], autoimmune arthritis[4], sepsis[5] and cancer[6], knowledge about its regulation is limited. Here we demonstrate that IgG1 immune complexes (ICs), the inhibitory IgG receptor FcγRIIB and the C-type lectin–like receptor dectin-1 suppress C5a receptor (C5aR) functions. IgG1 ICs promote the association of FcγRIIB with dectin-1, resulting in phosphorylation of Src homology 2 domain–containing inositol phosphatase (SHIP) downstream of FcγRIIB and spleen tyrosine kinase downstream of dectin-1. This pathway blocks C5aR-mediated ERK1/2 phosphorylation, C5a effector functions *in vitro* and C5a-dependent inflammatory responses *in vivo*, including peritonitis and skin blisters in experimental epidermolysis bullosa acquisita. Notably, high galactosylation of IgG N-glycans is crucial for this inhibitory property of IgG1 ICs, as it promotes the association between FcγRIIB and dectin-1. Thus, galactosylated IgG1 and FcγRIIB exert anti-inflammatory properties beyond their impact on activating FcγRs.

Activating FcγRs and C5aR promote inflammatory responses in experimental autoimmune nephritis[7,8], arthritis[9], IC alveolitis[10] and peritonitis[11]. C5a decreases the cellular activation threshold by upregulating the ratio of activating to inhibitory FcγRs (known as the A/I ratio)[10,11]. Activating FcγRs eventually drive proinflammatory effector functions[12]. C5a also recruits and activates inflammatory cells such as neutrophils, macrophages and mast cells independently of FcγRs[2]. FcR γ-chain–deficient (*Fcer1g*$^{-/-}$) mice express no functional activating FcγRs but do express the inhibitory FcγRIIB. These mice are protected from IC-mediated inflammation despite the presence of C5a. We hypothesized that one mechanism underlying such protection could be an anti-inflammatory property of IgG ICs suppressing C5a-mediated effector functions.

To test our hypothesis, we injected C5a into the peritoneal cavity of BALB/c wild-type (WT) or *Fcer1g*$^{-/-}$ mice. As expected, neutrophils were recruited into the peritoneum in both mouse strains (**Fig. 1a**). IgG1 is the most abundant isotype of serum antibody in mice. The preferential binding of IgG1 to inhibitory FcγRIIB is considered a protective mechanism to prevent incidental activation of circulating myeloid cells by binding of ICs to activating FcγRs[12]. Intravenous injection of the trinitrophenyl (TNP)-specific IC comprising IgG1 clone 107.3 and TNP-OVA (107.3-IC)[13] 30 min before C5a administration reduced C5a-mediated neutrophil migration into the peritoneum in WT and *Fcer1g*$^{-/-}$ mice but not in FcγRIIB-deficient (*Fcgr2b*$^{-/-}$) mice (**Fig. 1a** and **Supplementary Fig. 1**). Monomeric 107.3 antibody did not have an anti-inflammatory effect (data not shown). We have previously shown that the peritoneal inflammation induced by ovalbumin (OVA)-specific ICs is mediated by C5a[11]. Pretreatment with 107.3-IC blocked OVA-IC–induced peritonitis in WT but not *Fcgr2b*$^{-/-}$ mice, demonstrating a crucial role for FcγRIIB in 107.3-IC–mediated inhibition of C5a-dependent inflammation (**Fig. 1b**).

The mechanisms underlying C5aR-mediated extravasation and tissue recruitment of neutrophils involve the β_2 integrin heterodimer CD11b and CD18 (CR3)[14]. C5a upregulated CD11b expression on neutrophils from WT (data not shown) and *Fcer1g*$^{-/-}$ mice in a dose-dependent manner (**Supplementary Fig. 2**), and this upregulation was significantly reduced upon 107.3-IC pretreatment and was

[1]Institute for Systemic Inflammation Research, University of Lübeck, Lübeck, Germany. [2]Division of Cellular and Molecular Immunology, University of Cincinnati College of Medicine, Cincinnati, Ohio, USA. [3]Institute of Infection and Immunity, Cardiff University School of Medicine, Heath Park, Cardiff, UK. [4]Glycodesign and Glycoanalytics, Central Institute of Laboratory Medicine and Pathobiochemistry, Charité Medical University, Berlin, Germany. [5]Laboratory of Tolerance and Autoimmunity, German Rheumatism Research Center, Berlin, Germany. [6]Section of Infection and Immunity, University of Aberdeen, Aberdeen, UK. [7]Institute of Biology, Center for Structural and Cell Biology in Medicine, University of Lübeck, Lübeck, Germany. [8]Division of Emergency Medicine, University of Cincinnati College of Medicine, Cincinnati, Ohio, USA. [9]Department of Respiratory Diseases Research, Boehringer Ingelheim Pharma GmbH, Biberach, Germany. [10]Department of Dermatology, University of Lübeck, Lübeck, Germany. [11]Department of Biology, Chair of Genetics, University of Erlangen-Nuremberg, Erlangen, Germany. [12]Division of Immunology, University of Cincinnati College of Medicine, Cincinnati, Ohio, USA. [13]Department of Medicine, Cincinnati Veterans Affairs Medical Center Cincinnati, Ohio, USA. [14]These authors contributed equally to this work. Correspondence should be addressed to J.K. (joerg.koehl@uksh.de).

Received 11 October 2011; accepted 12 June 2012; published online 26 August 2012; doi:10.1038/nm.2862

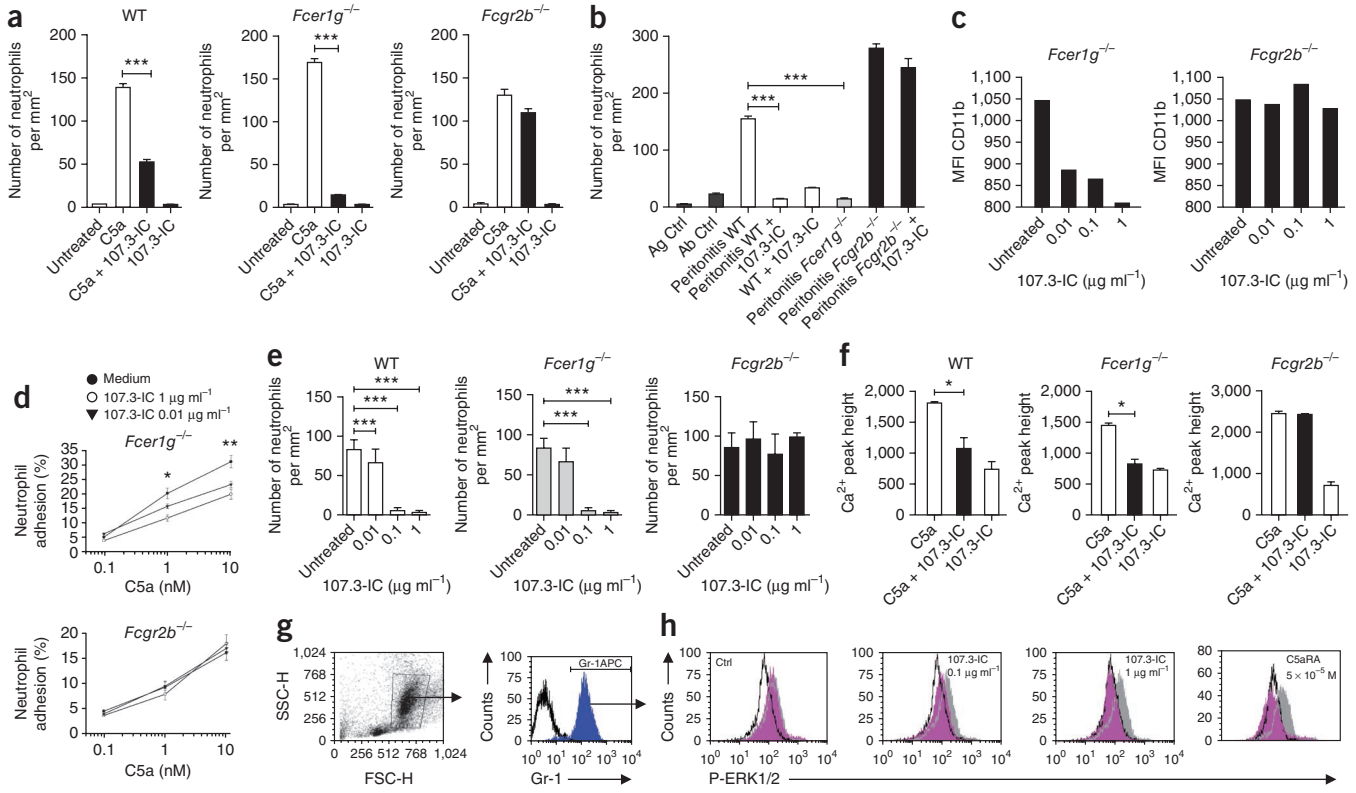

Figure 1 IgG1-ICs inhibit C5a-mediated inflammatory responses *in vivo* and *in vitro* by an FcγRIIB-dependent mechanism. (**a**,**b**) Peritoneal migration of neutrophils in response to C5a (**a**) or OVA-ICs comprising OVA and OVA-specific rabbit IgG (**b**) with or without 107.3-ICs in WT, *Fcer1g*$^{-/-}$ or *Fcgr2b*$^{-/-}$ mice. (**c**,**d**) Impact of 107.3-ICs on CD11b expression (**c**) and iC3b-dependent adhesion (**d**) in bone marrow–derived neutrophils from *Fcer1g*$^{-/-}$ and *Fcgr2b*$^{-/-}$ mice. MFI, mean fluorescence intensity. (**e**,**f**) C5a-mediated migration of bone marrow–derived neutrophils (**e**) and increase in $[Ca^{2+}]_i$ in bone marrow–derived cells (**f**) from WT, *Fcer1g*$^{-/-}$ or *Fcgr2b*$^{-/-}$ mice with or without 107.3-ICs. (**g**) Gating of bone marrow–derived neutrophils according to their cell size (FSC) and granularity (SSC) pattern (left dot plot) and the expression of the Gr-1 marker (histogram on the right). (**h**) Dose-dependent impact of 107.3-ICs on C5a-mediated ERK1/2 phosphorylation in Gr-1$^+$ WT bone marrow–derived neutrophils (three graphs on the left) and the effect of the C5a receptor antagonist A8$^{\Delta 71-73}$(C5aRA) on C5a-mediated ERK1/2 phosphorylation in bone marrow–derived neutrophils (graph on the right). Empty histogram, ERK phosphorylation in the absence of C5a (background); gray histogram, treatment with C5a (5×10^{-8} M; 1 min); magenta histogram, C5a (5×10^{-8} M; 1 min) + 107.3-ICs or C5aRA at the indicated concentrations. Results in **c** and **g** are representative of at least three independent experiments. Values in **a**,**b**,**d**–**f** are means ± s.e.m. (n = 5–10 per group). *$P < 0.05$, **$P < 0.01$, ***$P < 0.001$.

absent with cells from *Fcgr2b*$^{-/-}$ mice (**Fig. 1c**). 107.3-IC administration also reduced C5a-dependent neutrophil adhesion among cells from *Fcer1*$^{-/-}$ but not *Fcgr2b*$^{-/-}$ mice (**Fig. 1d**). Next, we found that 107.3-ICs dose-dependently inhibited C5a-mediated chemotaxis of bone marrow–derived neutrophils and peritoneal macrophages (**Fig. 1e** and **Supplementary Fig. 3a–d**) from WT and *Fcer1g*$^{-/-}$ mice but not from *Fcgr2b*$^{-/-}$ mice. Pharmacological targeting of FcγRIIB with the FcγRIIB-specific blocking antibody Ly17.2 abrogated the inhibitory effect of 107.3-ICs on C5a-mediated neutrophil migration (**Supplementary Fig. 4**). Thus, 107.3-ICs inhibit the functions not only of activating FcγRs[12] but also of complement-mediated acute inflammation. Moreover, we found that 107.3-ICs blocked not only C5aR but also CXCL2-dependent neutrophil migration of WT- and *Fcer1g*$^{-/-}$- but not *Fcgr2b*$^{-/-}$-derived cells (**Supplementary Fig. 3b**,**e**), suggesting a more general mechanism of inhibition.

C5aR exerts many of its biological functions through activation of the mitogen-activated protein (MAP) kinases extracellular signal-regulated kinases 1 and 2 (ERK1/2) and the phospholipase C–inositol phosphate pathway, leading to an increase in intracellular calcium release ($([Ca^{2+}]_i)^2$). 107.3-ICs blocked the C5a-mediated rise of $[Ca^{2+}]_i$ in bone marrow–derived cells from WT and *Fcer1g*$^{-/-}$ mice but not from *Fcgr2b*$^{-/-}$ mice (**Fig. 1f**). Next, we tested the impact of 107.3-ICs on C5a-mediated ERK1/2 phosphorylation in Gr1$^+$ bone marrow–derived neutrophils (**Fig. 1g**). C5a promotes phosphorylation of ERK1/2 in Gr1$^+$ bone marrow–derived neutrophils (**Supplementary Fig. 5a**), which is inhibited by 107.3-ICs in a dose-dependent manner in bone marrow–derived neutrophils from WT but not *Fcgr2b*$^{-/-}$ mice (**Fig. 1h** and **Supplementary Fig. 5b**). This inhibitory effect was similar in magnitude to what we found when C5aR signaling was blocked with the C5aR antagonist A8$^{\Delta 71-73}$ (5×10^{-5} M)[15] (**Fig. 1h**). Taken together, these results demonstrate that IgG1-ICs block C5a-mediated inflammation by an FcγRIIB-dependent mechanism leading to inhibition of both ERK1/2 phosphorylation and intracellular calcium release.

IgG1 IC-mediated coaggregation of FcγRIIB with activating FcγRs negatively regulates immune cell activation. Mechanistically, such coaggregation enables the Src kinase that phosphorylates the immunoreceptor tyrosine-based activation motif (ITAM) in the γ-chain of activating FcγRs to also phosphorylate the immunoreceptor tyrosine-based inhibitory motif (ITIM) within the α-chain of FcγRIIB[12]. The tyrosine-phosphorylated ITIM then allows binding and activation of SHIP. Because 107.3-ICs block C5a-mediated chemotaxis of myeloid cells from *Fcer1g*$^{-/-}$ mice, the effect does not result from classical pairing

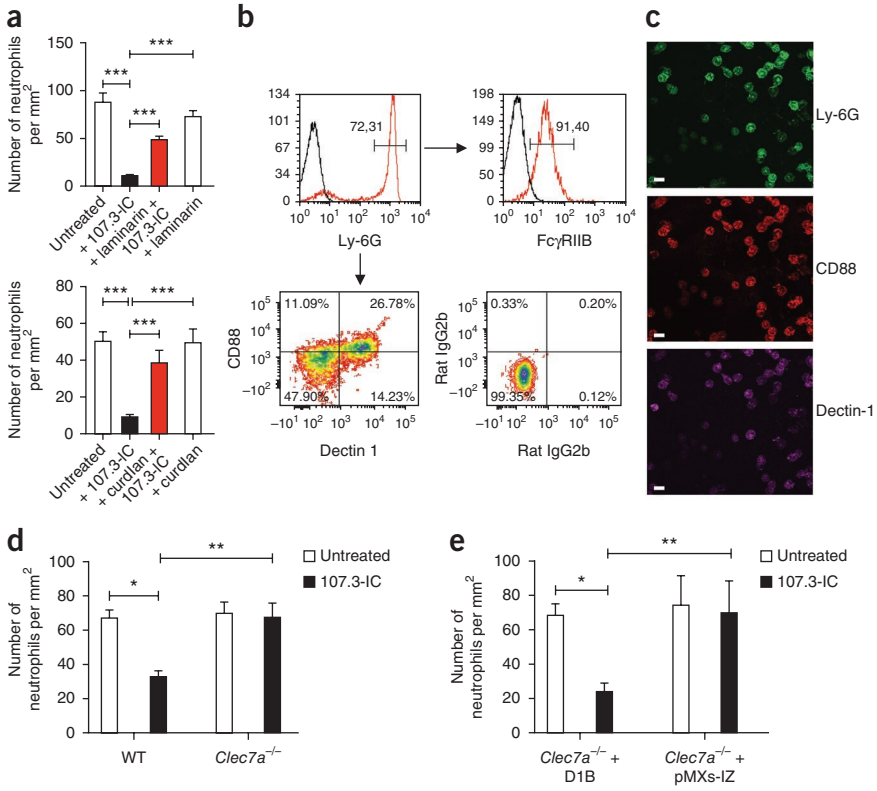

Figure 2 The inhibitory effect of IgG1-ICs on neutrophil migration depends on dectin-1. (**a**) Impact of 107.3-ICs on C5a-mediated migration of bone marrow–derived neutrophils *in vitro* when dectin-1 is blocked by pretreatment with laminarin (top) or curdlan (bottom) ($n = 3$ per group). (**b**) C5aR (CD88) and dectin-1 expression (bottom left contour plot; isotype control shown in the bottom right plot) on Ly-6G^{hi} bone marrow–derived neutrophils (top left histogram), as determined by flow cytometry. FcγRIIB expression of Ly-6G^{hi} neutrophils is shown in the top right histogram. (**c**) Bone marrow cells that migrated toward C5a (10^{-8} M for 30 min) were stained for membrane expression of Ly-6G, dectin-1 and C5aR and analyzed by confocal microscopy. All migrated cells are Ly-6G^{hi} neutrophils that express dectin-1 and C5aR. Scale bars, 10 μm. (**d**,**e**) Impact of 107.3-IC treatment on C5a-mediated chemotaxis of bone marrow–derived neutrophils from 129S6/SvEv WT mice and from *Clec7a*$^{-/-}$ mice (**d**) or a *Clec7a*$^{-/-}$ neutrophil cell line transfected with the dectin-1B isoform (D1B) or with vector alone (pMXs-IZ) (**e**) ($n = 3$ per group). Values are means ± s.e.m. $^{*}P < 0.05$, $^{**}P < 0.01$, $^{***}P < 0.001$.

of activating FcγRs with FcγRIIB. To search for potential new partners of FcγRIIB driving ITIM and SHIP phosphorylation, we focused on dectin-1 (gene symbol *Clec7a*), as it harbors an ITAM-like motif and is expressed on neutrophils[16]. First, we evaluated the impact of the dectin-1 inhibitor laminarin and the dectin-1 agonist curdlan on the inhibitory effect of 107.3-ICs. *In vitro* preincubation with laminarin or curdlan largely blocked the inhibitory effects of 107.3-IC inhibitory on C5a-mediated neutrophil migration, indicating that dectin-1 is required (**Fig. 2a**). The particulate β-glucan polymer curdlan but not the soluble polymer laminarin promotes rapid internalization of dectin-1 in neutrophils[17] (**Supplementary Fig. 6**), suggesting that the surface availability of dectin-1 is crucial for the inhibitory effect of IgG1-IC. We found that 30–40% of Ly-6G^{hi} bone marrow–derived neutrophils express dectin-1. C5aR expression follows the same pattern; that is, about 25–30% of Ly-6G^{hi} neutrophils express dectin-1and C5aR (**Fig. 2b**). About 10% of bone marrow–derived neutrophils are C5aR^{dim}dectin-1^{-}. FcγRIIB is expressed on almost all Ly-6G^{hi} neutrophils (**Fig. 2b**). In line with these findings, only Ly6G^{hi}dectin-1^{+}C5aR^{+} neutrophils migrated toward C5a (**Fig. 2c**). 107.3-ICs failed to inhibit C5a-mediated migration of bone marrow–derived neutrophils from dectin-1-deficient (*Clec7a*$^{-/-}$) mice[18] (**Fig. 2d**). C5a-mediated migration was, however, blocked by 107.3-ICs in *Clec7a*$^{-/-}$ neutrophils retrovirally transduced with the dectin-1B isoform but not with the control vector lacking dectin-1 (ref. 19) (**Fig. 2e** and **Supplementary Fig. 7**). Thus, IgG1-ICs require FcγRIIB and dectin-1 to inhibit C5a-mediated effector functions in neutrophils.

To search for the signaling pathways underlying this inhibitory effect of IgG1-ICs, we noted that the inhibitory effect occurred after 1 min and that inhibition of tyrosine phosphorylation by the tyrosine kinase inhibitor genistein completely abrogated the inhibitory effect of IgG1-IC (**Fig. 3a** and **Supplementary Fig. 8a**). Phosphorylated Src kinases mediate tyrosine phosphorylation of the FcγRIIB-associated ITIM and the ITAM-like motif in dectin-1. We found that the two Src-family kinase inhibitors I and II completely blocked the inhibitory effect of 107.3-ICs on neutrophil (**Fig. 3b**,**c**).

Ligation of dectin-1 results in the phosphorylation of spleen tyrosine kinase (Syk)[20]. Genetic deletion of Syk in inducible Syk-deficient mice[21] and pharmacological targeting by four different Syk kinase inhibitors, R406, piceatannol, BAY 61-3606 or Syk inhibitor, completely reversed the inhibitory effect of IgG1-ICs on C5a-mediated neutrophil chemotaxis (**Fig. 3d**,**e** and **Supplementary Figs. 8b–d** and **9**). To further demonstrate that IgG1-IC promotes Syk phosphorylation in a dectin-1–dependent manner, we pulled down phosphorylated Syk with a Syk-binding phosphopeptide[22] in the *Clec7a*$^{-/-}$ neutrophil cell line transduced with the dectin-1B isoform following 107.3-IC treatment (**Supplementary Fig. 8e**). Finally, by confocal microscopy, Syk (**Fig. 3f**) and SHIP (**Fig. 3g**) are phosphorylated in bone marrow–derived neutrophils from WT but not *Fcgr2b*$^{-/-}$ or *Clec7a*$^{-/-}$ mice in response to 107.3-IC treatment. Phosphorylated Syk or phosphorylated SHIP colocalize with FcγRIIB and dectin-1 in response to 107.3-IC administration (**Fig. 3f**,**g** and **Supplementary Movies 1–5**). Notably, 107.3-IC treatment resulted in rapid and transient Syk and SHIP phosphorylation within 1–3 min that declined after 5 min (**Supplementary Fig. 10a**,**b**).

Taken together, these data suggest that IgG1-ICs engage dectin-1, leading to Syk phosphorylation. Tyrosine and Syk phosphorylation downstream of dectin-1 are also linked to tyrosine phosphorylation of the ITIM within FcγRIIB and subsequent SHIP phosphorylation. This pathway then blocks C5a-mediated ERK1/2 phosphorylation and calcium influx crucial for C5a-mediated proinflammatory effector functions.

To identify the mechanism underlying the interaction of IgG1-ICs with dectin-1 and FcγRIIB, we focused on the Fc glycan composition. The N-glycan at Asn297 of the Fc moiety is essential for binding of IgG to FcγRs[23], the serum collectin mannose-binding lectin[24] and the

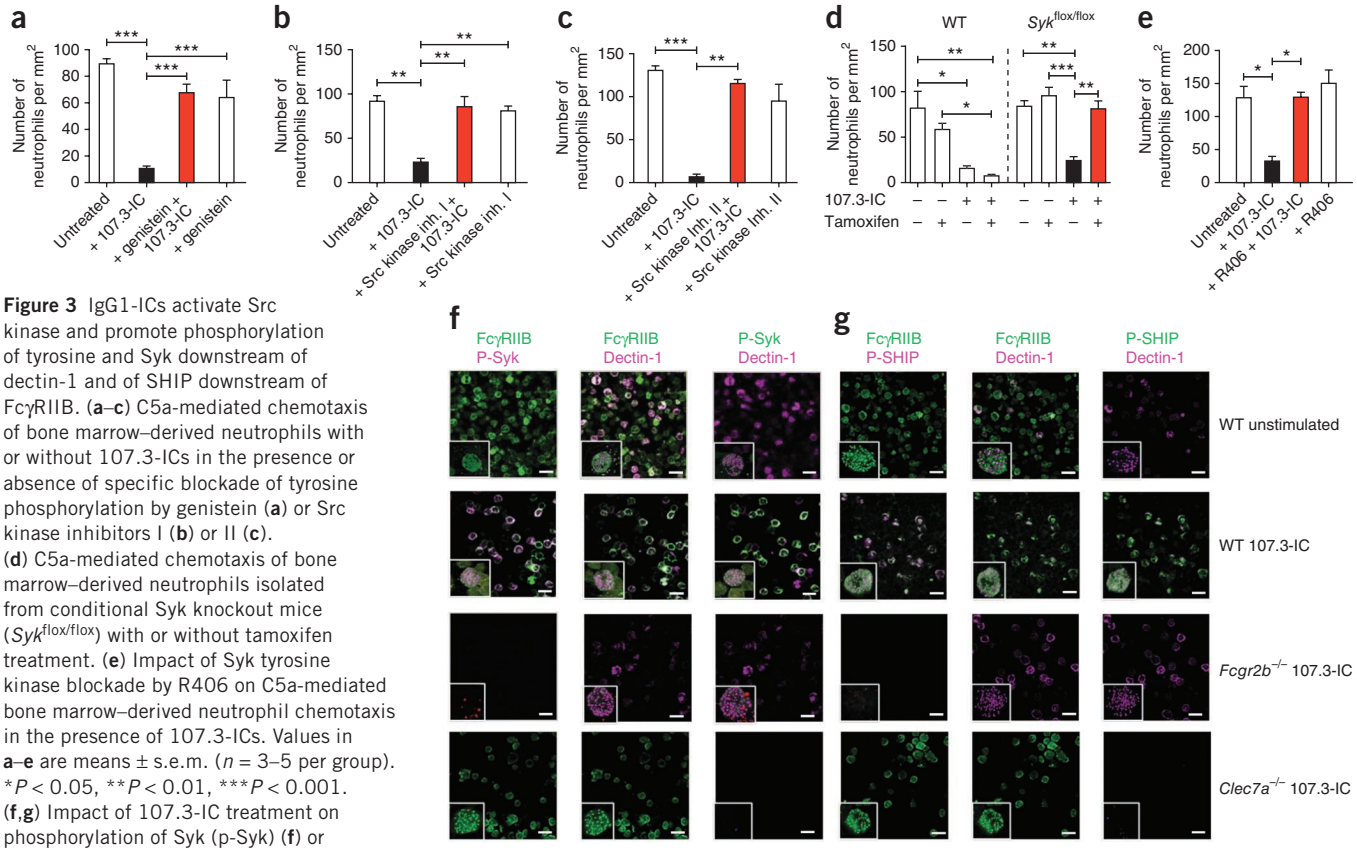

Figure 3 IgG1-ICs activate Src kinase and promote phosphorylation of tyrosine and Syk downstream of dectin-1 and of SHIP downstream of FcγRIIB. (**a**–**c**) C5a-mediated chemotaxis of bone marrow–derived neutrophils with or without 107.3-ICs in the presence or absence of specific blockade of tyrosine phosphorylation by genistein (**a**) or Src kinase inhibitors I (**b**) or II (**c**). (**d**) C5a-mediated chemotaxis of bone marrow–derived neutrophils isolated from conditional Syk knockout mice ($Syk^{flox/flox}$) with or without tamoxifen treatment. (**e**) Impact of Syk tyrosine kinase blockade by R406 on C5a-mediated bone marrow–derived neutrophil chemotaxis in the presence of 107.3-ICs. Values in **a**–**e** are means ± s.e.m. ($n = 3$–5 per group). $^*P < 0.05$, $^{**}P < 0.01$, $^{***}P < 0.001$. (**f**,**g**) Impact of 107.3-IC treatment on phosphorylation of Syk (p-Syk) (**f**) or SHIP (p-SHIP) (**g**) in bone marrow–derived neutrophils from WT, *Fcgr2b*$^{-/-}$ or *Clec7a*$^{-/-}$ mice. Depicted are immunofluorescence signals in the absence of 107.3-ICs (first rows) or obtained 3 min after incubation with 107.3-ICs (second, third and fourth rows). Co-localization of p-Syk and p-SHIP with FcγRIIB and dectin-1 in response to 107.3-IC treatment is demonstrated by white fluorescent neutrophils in the second rows. The insets show colocalization (white spots) using Z-stacks of images acquired by confocal microscopy and IMARIS image analysis software and the IsoSurface feature. Results are representative of two (*Clec7a*$^{-/-}$) or three independent experiments. Scale bars, 20 μm.

collectin-related molecule C1q[25]. Dectin-1 recognizes β-1,3-glucans expressed by a broad range of fungal pathogens[26]. However, dectin-1 has not be shown to interact with any Fc glycan. A recent nuclear magnetic resonance analysis demonstrated that Fc glycan is more dynamic and accessible than previously thought[27]. When we determined the N-glycan galactosylation (**Supplementary Fig. 11**) of the 107.3 antibody by MALDI-TOF, we observed 81.8% glycan galactosylation. The N-glycan galactosylation of two other TNP-specific IgG1 antibodies, 7B4 and H5 (ref. 28), was only 24.6% and 29.7%, respectively (**Supplementary Fig. 12** and **Supplementary Table 1**). IgG1-ICs composed of 7B4 or H5 antibody did not inhibit C5a-mediated chemotaxis of bone marrow neutrophils (**Supplementary Fig. 13a**). To directly assess the importance of N-glycan galactosylation, we galactosylated or degalactosylated H5 antibody *in vitro*, yielding a highly galactosylated form (HiGalH5-Ab; Fc glycan galactose content 96.9%) and a degalactosylated form (LoGalH5-Ab; Fc glycan galactose content 8.8%) (**Supplementary Fig. 12** and **Supplementary Table 1**). N-glycan composition had no effect on antigen binding (**Supplementary Fig. 14**). Immune complexes comprised of HiGalH5 (HiGalH5-ICs) but not LoGalH5-ICs inhibited the C5a-mediated chemotaxis, CD11b upregulation and increase in $[Ca^{2+}]_i$ among bone marrow–derived neutrophils from WT and *Fcer1g*$^{-/-}$ mice but not from *Fcgr2b*$^{-/-}$ or *Clec7a*$^{-/-}$ mice (**Supplementary Fig. 13a**–**c**). Additional sialylation of highly galactosylated H5 antibody (SialH5) (**Supplementary Fig. 12** and **Supplementary Table 1**) did not alter the inhibitory effect (**Supplementary Fig. 15a**). Notably, highly galactosylated TNP-specific IgG2a-ICs did not block C5a-mediated chemotaxis *in vitro*, suggesting that not only the glycan composition but also the IgG isotype, that is, IgG1, contributes to the inhibitory effect (**Supplementary Fig. 15a**–**c**).

In vivo, HiGalH5-ICs but not LoGalH5-ICs almost completely suppressed C5a-mediated neutrophil recruitment into the peritoneum of WT but not *Fcgr2b*$^{-/-}$ or *Clec7a*$^{-/-}$ mice (**Fig. 4a**). Further, intravenous administration of curdlan resulted in internalization of dectin-1 on recruited neutrophils and abrogated the inhibitory effect of HiGalH5-ICs on C5a-mediated neutrophil recruitment into the peritoneum (**Fig. 4b** and **Supplementary Fig. 16**). Previous data suggest a key role for C5 in an experimental model of epidermolysis bullosa acquisita (EBA)[29], a subepidermal autoimmune blistering disease induced by the transfer of rabbit IgG directed against mouse type VII collagen. We found that *C5ar1*$^{-/-}$ mice were protected from the development of EBA (**Supplementary Fig. 17**). HiGalH5-IC but not LoGalH5-IC treatment reduced the development of cutaneous lesions in this model (**Fig. 4c**,**d** and **Supplementary Fig. 18**). HiGal-ICs were not protective in *Clec7a*$^{-/-}$ mice, confirming the key role of dectin-1 in the protective effect of HiGal-ICs (**Supplementary Fig. 19**). Although dectin-1–deficient humans and mice do not develop spontaneous autoimmunity, our data suggest that dectin-1 may aggravate the inflammatory effector response in autoimmune diseases mediated by C5a. In line with this view, data

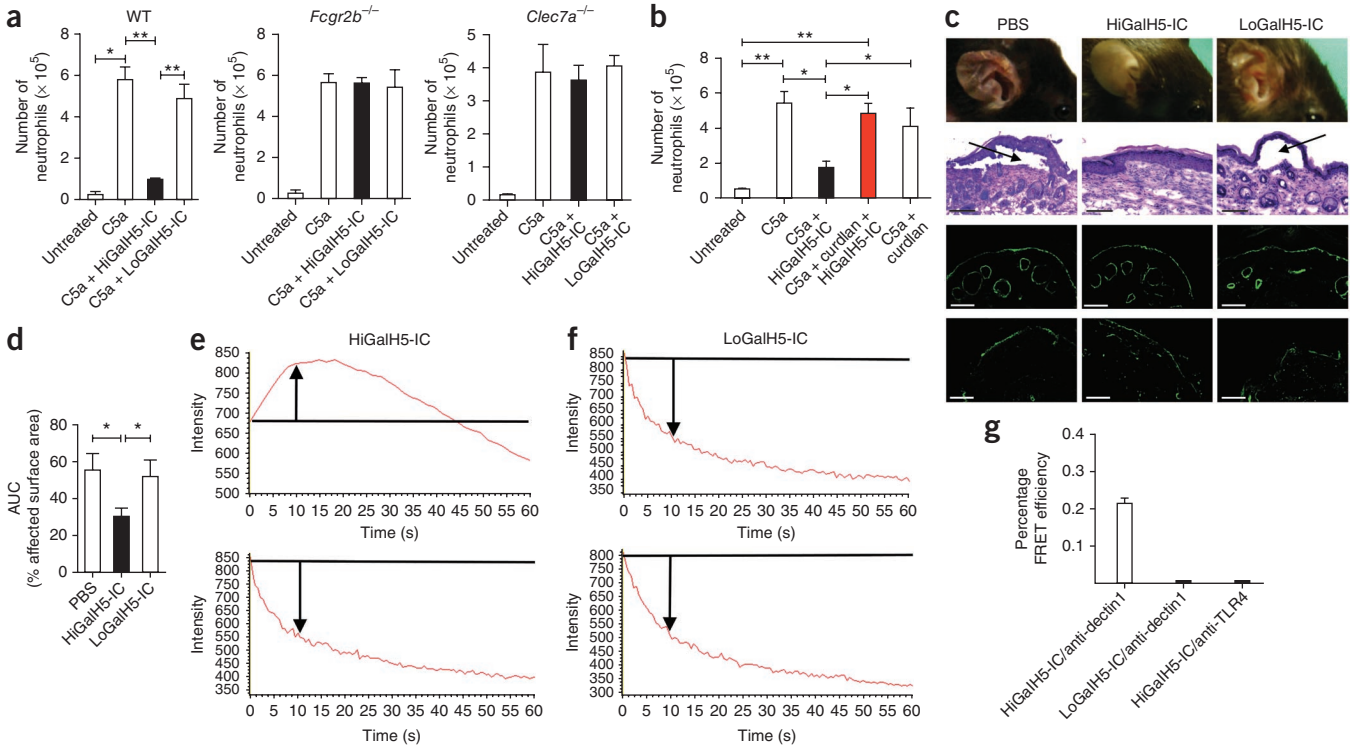

Figure 4 High Fc glycan galactosylation is crucial for the inhibitory effect of IgG1-ICs *in vivo* and promotes the association of FcγRIIB and dectin-1. (**a**) Peritoneal migration of neutrophils in response to C5a with or without 107.3-ICs in WT, *Fcgr2b*$^{-/-}$ or *Clec7a*$^{-/-}$ mice ($n = 5$ per group). (**b**) Impact of curdlan pretreatment on peritoneal neutrophil migration in response to intraperitoneal (i.p.) injection of C5a with or without HiGalH5-ICs ($n = 5$ per group). (**c**) Development of cutaneous lesions (first row), subepidermal split formation (second row), linear deposition of rabbit antibody to type VII collagen (third row) and C3 (fourth row) at the basement membrane in experimental EBA (day 12) in PBS, HiGalH5-IC and LoGal-H5-IC treatment groups. Black arrows point toward dermal-epidermal separation. Scale bars, 100 μm. (**d**) Clinical disease severity in PBS-, LoGalH5IC– and HiGalH5-IC–treated mice during the course of experimental EBA (days 4–12), as quantified by assessment of the area under the curve (AUC); values in **a**,**b**,**d** are means ± s.e.m. $^{*}P < 0.05$, $^{**}P < 0.01$. (**e**,**f**) Time-dependent change in fluorescence intensity of Cy3-HiGalH5-ICs (**e**) and Cy3-LoGalH5-ICs (**f**) donors during dectin-1–specific antibody conjugated to Alexa647 acceptor photobleach in the presence (top images) or absence (bottom images) of acceptor staining on bone marrow cells. Arrows indicate the change of fluorescence intensity as compared with the starting value (marked by the black line). (**g**) FRET efficiency following acceptor bleaching in bone marrow cells treated with either Cy3-HiGalH5-ICs ($n = 30$) or Cy3-LoGalH5-ICs ($n = 20$) as donor and dectin-1–specific antibody conjugated to Alexa647 as acceptor. As a negative control ($n = 10$), Cy3-HiGalH5-ICs were used as donor and TLR4-specific antibody conjugated to Alexa647 as acceptor. Values in **g** are means ± s.e.m.

from experimental models of autoimmune arthritis[30] or encephalitis models[31] point toward a role for dectin-1 as a modulator of autoimmune-driven inflammation.

To directly assess whether N-glycan galactosylation drives the association of FcγRIIB and dectin-1, we performed a two-step approach. First, we found that HiGalH5-ICs, H5-ICs and/or LoGalH5-ICs bind FcγRIIB-transfected Chinese hamster ovary cells (**Supplementary Fig. 20**) and to recombinant mouse FcγRIIB-Fc (**Supplementary Fig. 21**) with similar affinities. In contrast, such ICs do not bind recombinant dectin-1–Fc or a dectin-1–transfected T cell lymphoma cell line (BWZ cells) (data not shown). These data demonstrate that in the absence of FcγRIIB, IgG1-ICs do not bind dectin-1 independent of their galactosylation status. In a second approach, we found by Förster resonance energy transfer (FRET) that HiGalH5-ICs but not LoGalH5-ICs promotes the association of FcγRIIB with dectin-1. Using Cy3-labeled HiGalH5-ICs as donor and an Alexa647-labeled dectin-1–specific antibody as acceptor, we found a FRET efficiency of 20% (**Fig. 4e–g** and **Supplementary Fig. 22**). Notably, we found no FRET when we used Cy3-LoGalH5-ICs as donor or Cy3-HiGalH5-ICs as donor and an Alexa647-labeled Toll-like receptor 4–specific antibody as acceptor (**Fig. 4e–g**).

Collectively, our findings demonstrate that high N-glycan galactosylation of IgG1 molecules promotes cooperative signaling of the FcγRIIB with dectin-1, resulting in an inhibitory signaling pathway that blocks the proinflammatory effector functions of the chemoattractant GPCRs C5aR and CXCR2 (**Supplementary Fig. 23**). This mechanism is distinct from the anti-inflammatory properties mediated by sialylation of Fc-linked N-glycans[32]. About 25–35% of Fc glycans from serum IgG are agalactosylated under steady-state conditions[33]. This frequency markedly increases in experimental and human autoimmune conditions, including rheumatoid arthritis, systemic lupus erythematosus, inflammatory bowel disease and infections[33]. Thus, the inhibitory effect of highly galactosylated IgG1-ICs may serve as a feedback loop to control complement and chemokine-mediated inflammation in autoimmunity and infection before IgGs switch to the proinflammatory agalactosyl glycoform. This effect may also contribute to the increased incidence of autoimmune phenomena in patients with hypogammaglobulinemia or common variable immunodeficiency[34].

METHODS

Methods and any associated references are available in the online version of the paper.

Note: Supplementary information is available in the online version of the paper.

ACKNOWLEDGMENTS

This work is supported by the German Research Foundation (Deutsche Forschungsgemeinschaft, GRK1727; project 8 and SFB/TR22; project A21) to J.K., EXC306/1 to D.Z., R.L. and J.K., and by Deutsche Forschungsgemeinschaft EH221-5 to M.E. P.R.T. is a Medical Research Council (UK) Senior Fellow (G0601617). G.D.B. was supported by the Wellcome Trust. We thank T. Köhli for technical assistance with the surface plasmon resonance analysis, T. Gutsmann for help with the fluorescence spectroscopy measurements, T. Peters and L. Wollin for helpful discussions and B. Heyman (Uppsala University, Sweden) for providing the H5 and the 7B4 hybridoma clones.

AUTHOR CONTRIBUTIONS

C.M.K. and M.K.P. conducted key studies and analyzed the data. J.F. assessed antigen binding of *in vitro*–glycosylated IgGs and performed phenotypical characterization of bone marrow cells, and some *in vivo* studies. R.K. and C.M.K. performed the EBA studies. R.L. and D.Z. provided the rabbit collagen type VII–specific IgG for the EBA studies and helped with EBA-related data analysis. P.R.T., M.R. and J.U.M. provided the dectin-1–transduced neutrophil and macrophage cell lines, and helped with assays using such lines. S.J.O. performed the peptide pull-down experiments. M.B., D.P. and V.B. did the MALDI-TOF analysis. A.W. and C.H. performed the *in vitro* galactosylation of the H5 antibody. G.D.B. and D.M.R. provided the *Clec7a*$^{-/-}$ mice and helped with the neutrophil assays using such mice and with *ex vivo* assays with primary *Clec7a*$^{-/-}$ cells. I.V.M. provided material and advice for the FRET experiments. R.T.S. and F.D.F. provided TNP-OVA and helped with initial IC studies. N.L.H. and G.K. performed the ERK phosphorylation studies with neutrophils. E.W. provided the conditional Syk-knockout mice and the protocol for *in vitro* Syk depletion. F.N. provided the recombinant IgG1 7B4 antibody and recombinant mouse FcγRIIB-Fc and assessed HiGalH5-IC and H5-IC binding to FcγRIIB-transfected Chinese hamster ovary cells. M.E. provided scientific input and coordinated the glycan analysis. J.K. designed and coordinated the study, analyzed the data and wrote the manuscript.

COMPETING FINANCIAL INTERESTS

The authors declare competing financial interests: details are available in the online version of the paper.

Published online at http://www.nature.com/doifinder/10.1038/nm.2862.
Reprints and permissions information is available online at http://www.nature.com/reprints/index.html.

1. Ricklin, D., Hajishengallis, G., Yang, K. & Lambris, J.D. Complement: a key system for immune surveillance and homeostasis. *Nat. Immunol.* **11**, 785–797 (2010).
2. Klos, A. *et al.* The role of the anaphylatoxins in health and disease. *Mol. Immunol.* **46**, 2753–2766 (2009).
3. Köhl, J. *et al.* A regulatory role for the C5a anaphylatoxin in type 2 immunity in asthma. *J. Clin. Invest.* **116**, 783–796 (2006).
4. Hashimoto, M. *et al.* Complement drives T_H17 cell differentiation and triggers autoimmune arthritis. *J. Exp. Med.* **207**, 1135–1143 (2010).
5. Rittirsch, D. *et al.* Functional roles for C5a receptors in sepsis. *Nat. Med.* **14**, 551–557 (2008).
6. Markiewski, M.M. *et al.* Modulation of the antitumor immune response by complement. *Nat. Immunol.* **9**, 1225–1235 (2008).
7. Clynes, R., Dumitru, C. & Ravetch, J.V. Uncoupling of immune complex formation and kidney damage in autoimmune glomerulonephritis. *Science* **279**, 1052–1054 (1998).
8. Wenderfer, S.E. *et al.* C5a receptor deficiency attenuates T cell function and renal disease in MRLlpr mice. *J. Am. Soc. Nephrol.* **16**, 3572–3582 (2005).
9. Ji, H. *et al.* Arthritis critically dependent on innate immune system players. *Immunity* **16**, 157–168 (2002).
10. Shushakova, N. *et al.* C5a anaphylatoxin is a major regulator of activating versus inhibitory FcγRs in immune complex–induced lung disease. *J. Clin. Invest.* **110**, 1823–1830 (2002).
11. Godau, J. *et al.* C5a initiates the inflammatory cascade in immune complex peritonitis. *J. Immunol.* **173**, 3437–3445 (2004).
12. Nimmerjahn, F. & Ravetch, J.V. Fcγ receptors as regulators of immune responses. *Nat. Rev. Immunol.* **8**, 34–47 (2008).
13. Strait, R.T., Morris, S.C. & Finkelman, F.D. IgG-blocking antibodies inhibit IgE-mediated anaphylaxis *in vivo* through both antigen interception and FcγRIIb cross-linking. *J. Clin. Invest.* **116**, 833–841 (2006).
14. Jones, S.L., Knaus, U.G., Bokoch, G.M. & Brown, E.J. Two signaling mechanisms for activation of $\alpha_M\beta_2$ avidity in polymorphonuclear neutrophils. *J. Biol. Chem.* **273**, 10556–10566 (1998).
15. Otto, M. *et al.* C5a mutants are potent antagonists of the C5a receptor (CD88) and of C5L2: position 69 is the locus that determines agonism or antagonism. *J. Biol. Chem.* **279**, 142–151 (2004).
16. Taylor, P.R. *et al.* The β-glucan receptor, dectin-1, is predominantly expressed on the surface of cells of the monocyte/macrophage and neutrophil lineages. *J. Immunol.* **169**, 3876–3882 (2002).
17. Goodridge, H.S. *et al.* Activation of the innate immune receptor dectin-1 upon formation of a 'phagocytic synapse'. *Nature* **472**, 471–475 (2011).
18. Taylor, P.R. *et al.* Dectin-1 is required for β-glucan recognition and control of fungal infection. *Nat. Immunol.* **8**, 31–38 (2007).
19. McDonald, J.U. *et al.* *In vivo* functional analysis and genetic modification of *in vitro*–derived mouse neutrophils. *FASEB J.* **25**, 1972–1982 (2011).
20. Rogers, N.C. *et al.* Syk-dependent cytokine induction by dectin-1 reveals a novel pattern recognition pathway for C type lectins. *Immunity* **22**, 507–517 (2005).
21. Wex, E. *et al.* Induced Syk deletion leads to suppressed allergic responses but has no effect on neutrophil or monocyte migration *in vivo*. *Eur. J. Immunol.* **41**, 3208–3218 (2011).
22. Dennehy, K.M., Klimosch, S.N. & Steinle, A. Cutting edge: NKp80 uses an atypical hemi-ITAM to trigger NK cytotoxicity. *J. Immunol.* **186**, 657–661 (2011).
23. Nimmerjahn, F. & Ravetch, J.V. Divergent immunoglobulin g subclass activity through selective Fc receptor binding. *Science* **310**, 1510–1512 (2005).
24. Malhotra, R. *et al.* Glycosylation changes of IgG associated with rheumatoid arthritis can activate complement via the mannose-binding protein. *Nat. Med.* **1**, 237–243 (1995).
25. Raju, T.S. Terminal sugars of Fc glycans influence antibody effector functions of IgGs. *Curr. Opin. Immunol.* **20**, 471–478 (2008).
26. Geijtenbeek, T.B. & Gringhuis, S.I. Signalling through C-type lectin receptors: shaping immune responses. *Nat. Rev. Immunol.* **9**, 465–479 (2009).
27. Barb, A.W. & Prestegard, J.H. NMR analysis demonstrates immunoglobulin G N-glycans are accessible and dynamic. *Nat. Chem. Biol.* **7**, 147–153 (2011).
28. Wernersson, S. *et al.* IgG-mediated enhancement of antibody responses is low in Fc receptor γ chain–deficient mice and increased in Fc γ RII–deficient mice. *J. Immunol.* **163**, 618–622 (1999).
29. Sitaru, C. *et al.* Induction of dermal-epidermal separation in mice by passive transfer of antibodies specific to type VII collagen. *J. Clin. Invest.* **115**, 870–878 (2005).
30. Yoshitomi, H. *et al.* A role for fungal β-glucans and their receptor dectin-1 in the induction of autoimmune arthritis in genetically susceptible mice. *J. Exp. Med.* **201**, 949–960 (2005).
31. Manicassamy, S. *et al.* Toll-like receptor 2–dependent induction of vitamin A–metabolizing enzymes in dendritic cells promotes T regulatory responses and inhibits autoimmunity. *Nat. Med.* **15**, 401–409 (2009).
32. Anthony, R.M., Wermeling, F., Karlsson, M.C. & Ravetch, J.V. Identification of a receptor required for the anti-inflammatory activity of IVIG. *Proc. Natl. Acad. Sci. USA* **105**, 19571–19578 (2008).
33. Arnold, J.N., Wormald, M.R., Sim, R.B., Rudd, P.M. & Dwek, R.A. The impact of glycosylation on the biological function and structure of human immunoglobulins. *Annu. Rev. Immunol.* **25**, 21–50 (2007).
34. Agarwal, S. & Cunningham-Rundles, C. Autoimmunity in common variable immunodeficiency. *Curr. Allergy Asthma Rep.* **9**, 347–352 (2009).

ONLINE METHODS

Reagents. Monoclonal phycoerythrin (PE)-labeled antibodies to CD11b (M1/70; 1:100), Ly-6G (1A8; 1:100) and Gr-1 (RB6-8C5; 1:100) were from BD Pharmingen; Alexa488-labeled FcγRIIB-specific antibody (Ly17.2; 1:500) was used as described[11]; Monoclonal antibody to F4/80 (Cl:A3-1; 1:100), Ly-6B.2-FITC (7/4; 1:100), dectin-1 (conjugated to allophycocyanin (APC) or Alexa647 (2A11); 1:20) and to CD88 (conjugated to PE or Alexa647 (10/92); 1:20) were from AbD Serotec. The Alexa647-labeled antibody to TLR4 (MTS510; 1:100) was from eBioscience. The antibodies to F4/80 and Ly-6B.2 were labeled with Phycolink Peridinin-chlorophyll-protein complex (PerCP)-labeling kit (Europa Bioproducts) as per the manufacturer's instructions; the rabbit antibodies to p-p44/42 MAP kinase (Thr202/Tyr204; 1:20), p-Syk (Tyr352; 1:20), p-SHIP1 (Tyr1020; 1:20), IgG (conjugated to horseradish peroxidase) and antibody to p-Syk (C87C1; 1:20) were from Cell Signaling; the antibody to Syk was from Novus Biologicals. Streptavidin–Alexa Fluor 405 (SAv-Alexa405; 1:20), TSA detection kit Alexa Fluor 546, Fluo-4-AM and zeocin were from Invitrogen. The FITC-labeled pig antibody to rabbit IgG was from Dako (1:100). Diff-Quick staining solution was from Baxter, Merz & Dade. The goat antibody to C3 was from MP Biomedicals (1:100). The C5a receptor antagonist $A8^{\Delta 71-73}$ has been described elsewhere[15]. The mouse TNP-specific IgG 107.3 was from BD Pharmingen. The mouse TNP-specific IgG1 7B4 was generated by switching the original TNP-specific IgG2a to IgG1 and was produced by transient transfection in HEK293 cells as described[28]. The TNP-specific mouse IgG2a 7B4 was produced from hybridoma cells. Recombinant human C5a (rhC5a), Calcein, 4-hydroxytamoxifen, genistein, piceatannol and R406 were from Sigma-Aldrich. The Src kinase inhibitors I and II and Syk inhibitors and BAY 61-3606 were from Calbiochem. Poly-L-lysine–coated microtiter plates were from Corning. Laminarin, curdlan, stem cell factor (SCF) and β-estradiol were from Sigma-Aldrich. Interleukin-3 (IL-3) and IL-6 were from Peprotech. Mouse FcγRIIB-Fc and CHO-mFcγRIIB were used as described[35]. TNP-coupled BSA was from Biosearch Technology. Supplemented RPMI 1640 medium was from PAA laboratories. Fluoromount-G was from SouthernBiotech. Cy3 Amersham CyDye Antibody Labeling Kit was from GE Healthcare. The polyvinylidene fluoride membrane was from Millipore.

Mice. Female BALB/c or C57BL/6 mice were purchased from the Jackson Laboratory (Bar Harbor, ME). *Fcer1g*$^{-/-}$ and *Fcgr2b*$^{-/-}$ mice (on BALB/c background) were purchased from Taconic (Laven, Denmark). Dectin-1–deficient mice on the isogenic 129S6/SvEv background (129S6/SvEv.*Clec7a*$^{-/-}$), the C57BL/6 background (C57BL/6.*Clec7a*$^{-/-}$), and the 129S6/SvEv and the C57BL/6 control mice were obtained from our own breeding colonies. Dectin-1 deficiency was also backcrossed for eight generations onto the C57BL/6 genetic background for the production of cell lines (see below). C57BL/6.*Clec7a*$^{-/-}$ mice were used in peritonitis and in chemotaxis experiments with naive H5, HiGalH5-ICs and LoGalH5-ICs. Inducible Syk-knockout mice have recently been described[21] and were bred at Charles River. All mice were used at 8–12 weeks of age and handled in accordance with the appropriate institutional and national guidelines. All mouse studies were reviewed and approved by local authorities of the Animal Care and Use Committee (Ministerium für Landwirtschaft, Umwelt und ländliche Räume, Kiel, Germany) and performed by certified personnel.

Chemotaxis assay. Bone marrow–derived cells or peritoneal macrophages were resuspended in chemotaxis medium (GBSS containing 2% BSA) at a density of 5×10^6 cells ml^{-1}. The chemoattractants C5a (10^{-8} M) or CXCL2 (10^{-7} M) were diluted in chemotaxis medium, placed in the bottom wells of a micro Boyden chemotaxis chamber (Neuroprobe) and overlaid with a 3-μm polycarbonate membrane. Then, 50 μl of the cells were placed in the top wells and incubated for 30 min at 37 °C. In some experiments, cells were treated with the indicated concentrations of monomeric IgG1 or IgG1-ICs, IgG2a-ICs, the tyrosine phosphorylation inhibitor genistein (100 μM), the Src-family kinase inhibitors I and II (at 10 μM) or the Syk inhibitors piceatannol (100 μM), R406 (10 μM), Syk inhibitor (10 μM) or BAY 61-3606 (10 μM). Subsequently, the membranes were removed and the cells on the bottom side of the membrane were stained with Diff-Quick. The numbers of migrated cells in five high-power fields were counted, and the number of cells per mm^2 was calculated by computer assisted light microscopy. Results are expressed as the mean value of triplicate samples.

Preparation of TNP-OVA and of TNP-OVA/anti–TNP-OVA IgG1 immune complexes. TNP-OVA complexes were generated as described[13]. Briefly, 1 g of OVA was dissolved in 5 ml of saline and mixed with 500 μl 1 M $NaHCO_3$ pH 9.6. Then, 50 mg of TNP-ε-aminocaproyl-succinimide ester (OSU) was dissolved in 500 μl DMSO resulting in 100 mg/ml^{-1} TNP-OSU, which was added to the OVA solution and incubated overnight. The final TNP/OVA ratio was 10:4. TNP-OVA complexes were incubated with TNP-specific IgG1 antibodies at different ratios, and IC formation was determined by Ouchterlony gel diffusion.

C5a-mediated peritoneal inflammation. Mice were injected with C5a (200 nM, 100 μl, i.p.). After 6 h, mice were killed and neutrophil numbers in peritoneal lavage fluid were determined by Diff-Quick staining of Cytospin slides. At least >20 different microscopic fields were evaluated as described[11]. In some experiments, Ly-6G^{hi} neutrophil numbers were enumerated by flow cytometry using BD True count beads. In some experiments, mice were pretreated intravenously (i.v.) with 107.3-ICs (0.5–50 μg per kg body weight), HiGal H5-ICs or LoGalH5-ICs (50 μg per kg body weight).

Immune complex peritonitis. We used the reverse passive Arthus reaction model. Ovalbumin (OVA, 20 mg per kg body weight; Sigma) was injected i.v., followed by an i.p. injection of OVA-specific rabbit IgG (800 μg per mouse; ICN Biomedicals) as described[11]. Mice were killed 6 h after injury, and the peritoneal cavity was lavaged with 10 ml of PBS. Peritoneal cells were washed once with PBS, and 10^5 cells in 200 μl of PBS were used for preparation of cytospin slides. Neutrophil numbers were evaluated as outlined above. In some experiments, mice were pretreated i.v. with 107.3-ICs at a concentration of 50 μg per kg body weight.

Generation and purification of pathogenic type VII collagen–specific antibodies. Rabbits were immunized with recombinant forms of the NC1 domain of mouse type VII collagen as described[29]. IgGs from immune and normal rabbit sera were purified by affinity chromatography using protein G affinity as previously reported[29]. Isolated IgG was further subjected to affinity purification using recombinant His-tagged fragments of mouse type VII collagen (amino acids 757-967) and Affi-Gel affinity chromatography (Bio-Rad Lab). Reactivity of the isolated IgG fractions was confirmed by immunofluorescence microscopy on mouse skin before *in vivo* use.

Experimental epidermolysis bullosa acquisita model. Induction of experimental EBA followed published protocols[29] with minor modifications. Briefly, EBA was induced by a total of three subcutaneous injections of 100 μg rabbit type VII collagen–specific, affinity-purified IgG every second day. For treatment, i.v. injections of either PBS, HiGalH5-ICs, LoGalH5-ICs or 107.3-ICs (50 μg per kg body weight) were started on day –1 and repeated on days 3 and 6. Disease progression was evaluated over a time period of 12 d. On days 4, 7 and 12, disease severity was determined and expressed as percentage of body surface area affected by skin lesions, and tail biopsies were taken. On day 12, additional tissue samples were obtained for histological analyses. Disease outcome of the different treatment groups was compared by calculation of the area under the curve (AUC) obtained for the disease progression at the different time points, taking both disease onset and maximal disease activity into account.

Histopathology and immunofluorescence microscopy. Tissue samples were used for histopathological assessment and immunofluorescence microscopy as described previously[29]. To assess morphological skin alteration in diseased mice, sections were stained with H&E. IgG and C3 deposits were detected by direct immunofluorescence microscopy using an FITC-labeled pig anti-rabbit IgG antibody and goat anti-mouse C3 antibody.

Neutrophil preparation. Mice were killed by cervical dislocation under anesthesia. Femurs, tibias and humeri were removed, placed in PBS on ice

and subsequently flushed with PBS. More than 80% of cells isolated were polymorphonuclear cells, as defined by Diff-Quick staining, and stained positive for the Ly-6G marker. For Syk depletion in neutrophils from *Syk*$^{flox/flox}$ mice, cells were cultured in RPMI 1640 medium supplemented with 2 mM L-glutamine, 100 U/ml benzylpenicillin and 0.1 mg/ml dihydrostreptomycin (pen/strep) and 10% FCS in the presence 0.6 μM 4-hydroxy-tamoxifen in ethanol for 48 h. Controls were treated accordingly with ethanol only. Viability was determined by trypan blue exclusion and 7-AAD staining using a BD LSR II flow cytometer. Forty-eight hours of treatment with 4-hydroxy-tamoxifen did not affect the viability of bone marrow–derived neutrophils.

Macrophage preparation. To obtain mouse peritoneal macrophages, the peritoneal cavity was gently flushed with 5 ml of sterile PBS. Peritoneal cells were allowed to adhere on plastic microtiter plates for 4 h at 37 °C. Nonadherent cells were removed by several washing steps with PBS and adherent cells were used for cell migration. Flow cytometric analysis revealed that the majority of adherent cells were F4/80^{high}CD11b^{high}.

C5a-induced upregulation of CD11b expression. Neutrophils (1×10^6) were suspended in 100 μl of GBSS buffer containing 2% BSA and treated with C5a (10 nM) at 37 °C for 10 min. Then, cells were placed on ice and washed once with ice-cold PBS. For flow cytometric analysis of CD11b expression, Fc receptors were blocked with 2.4G2 antibody (BD Pharmingen; 1 μg per 10^6 cells in 100 μl of FACS buffer for 30 min on ice). Cells were washed once with PBS and then stained with anti-CD11b antibody conjugated to PE or the corresponding isotype control for 45 min on ice. Data were collected and analyzed on a FACSCalibur (Becton Dickinson) using FCS Express software (Version 3.0).

Complement receptor 3–mediated cell adhesion assay. Complement (iC3b)-coated surfaces were prepared by incubation of poly-L-lysine precoated plates with human IgM (10 μg ml^{-1}) and 10% human serum as described[36]. Bone marrow cells were labeled with calcein (2 μg ml^{-1}) for 30 min and added to the complement-coated surface ± C5a (0.1, 1 or 10×10^{-9} M) for 10 min at 37 °C. In some experiments, calcein-labeled cells were preincubated with 107.3-ICs (0.1 or 1 μg ml^{-1}) for 30 min at 37 °C. The fluorescence was measured using an FLX800 Microplate Fluorescence Reader (BioTek Instruments) before and after washing twice with PBS. The percentage adhesion was calculated by dividing the fluorescence signal remaining after washing by that observed before washing.

Increase in intracellular calcium $[Ca^{2+}]_i$. Bone marrow–derived cells were collected and loaded with 5 μM of the Ca^{2+}-sensitive fluorophore Fluo-4-AM (Invitrogen) for 30 min. Non-incorporated dye was washed away using PBS. Cells were then gated on Ly-6G^{hi} cells and analyzed on an LSRII flow cytometer (BD). The background signal was recorded for 30 s. Then C5a was added (10 nM), and recording was continued for another 90 s. The increase in $[Ca^{2+}]_i$ was calculated by assessment of the Ca^{2+} peak using the kinetic plug-in tool of the FlowJo software (Ver. 7.5, Tree Star).

Analysis of ERK1/2 phosphorylation. Bone marrow–derived cells from WT mice were cultured ± 107.3-ICs (0.1 or 1 μg ml^{-1}) or the C5aR antagonist A8$^{\Delta 71-73}$ for 30 min at 37 °C. Bone marrow–derived cells were then stimulated with C5a (50 nM) for 1 min and subsequently analyzed for ERK1/2 phosphorylation by intracellular staining with a rabbit anti-phospho-p44/42 MAP kinase antibody. In some experiments, bone marrow–derived cells from *Fcgr2b*$^{-/-}$ mice were used.

***In vitro* generation of neutrophils.** Bone marrow–derived cells were pooled from the femurs of female C57BL/6.*Clec7a*$^{-/-}$ mice and were depleted of lineage (lin)$^+$ cells using the mouse lineage cell depletion kit (Miltenyi Biotec) as directed by the manufacturer. The lin$^-$ cells were prestimulated with IL-3, IL-6 and SCF for 3 d as described[37] before being infected with the pMXs-IP:FL-ER-Hoxb8 retrovirus[19] and then immediately cultured in SCF and β-estradiol to bias toward neutrophil progenitor outgrowth. Two days after infection cells were selected in 1.5 μg/ml of puromycin for 10 d. Typically, this resulted in the production of stable precursors, termed Myeloid Precursor Hoxb8 from C57BL/6 (MyPH8-B6). The cells were maintained in SCF and β-estradiol as described[37]. MyPH8-B6.*Clec7a*$^{-/-}$ cells were reconstituted with the dectin-1B isoform with specific (pMXs-IZ:dectin-1B) or empty control (pMXs-IZ) retrovirus as previously described[38], but using MyPH8 culture medium supplemented with 50 μg/ml of zeocin to maintain the reconstituted cells. Expression of dectin-1B was verified by flow cytometry. For *in vitro* generation of neutrophils, MyPH8-B6.*Clec7a*$^{-/-}$:pMXs-IZ or MyPH8-B6.*Clec7a*$^{-/-}$:dectin-1B were washed three times with medium to remove the β-estradiol before differentiation for 4 d in SCF and granulocyte colony–stimulating factor (both 20 ng ml^{-1}). By day 4, neutrophils routinely represent 90–98% of the cells present and are identified by flow cytometry as Ly-6B.2^{high}CD117^{low} cells and on Cytospin preparations by their typical nuclear morphology.

Peptide pull-down and western blotting. The cells were serum starved for 30 min at 37 °C. Ten million were resuspended in 100 μl DPBS and stimulated at 37 °C with 10 μg IgG1-ICs for the indicated times. Cells were lysed with RIPA lysis buffer (50 mM Tris-HCl pH 7.4, 150 mM NaCl, 1% IGEPAL-CA-630, 0.25% Na-deoxycholate, 1 mM EDTA, Na_3VO_4, leupeptin, aprotinin and phenylmethylsulfonyl fluoride). For peptide pull-down experiments using a previously described biotinylated phosphopeptide[22] derived from Clec-2 (pClec2: MQDEDGpYITLNIKNK-biotin, Peptide Protein Research), cell lysates were incubated with 20 μg of peptide bound to streptavidin agarose beads (Life Technologies) for 4 h. Peptide pull-downs were washed, reducing Laemmli buffer was added and samples were heated for 5 min at 95 °C. Samples were separated by SDS-PAGE, transferred to PVDF membrane and analyzed by western blotting with anti-pSyk and anti-Syk antibodies.

Immunofluorescence staining of bone marrow–derived neutrophils. Neutrophils were preincubated for different time periods (1, 3 or 5 min) with or without IgG1-ICs at 37 °C. Cells were then fixed with BD Cytofix/Cytoperm (BD Bioscience). Phospho-Syk or phospho-SHIP antibodies were added, and the cells were incubated at 4 °C for 24 h. Cells were washed and then stained for phospho-Syk detection with an Alexa568-labeled secondary antibody, or, in the case of SHIP, using the tyramide signal amplification kit as described by the manufacturer (Invitrogen). For FcγRIIB and dectin-1 staining, samples were further incubated with Alexa488-labled FcγRIIB-specific and/or APC-dectin-1–specific Abs for 15 min at 4 °C. Cells were then mounted with Fluoromount-G. Images were obtained using the Olympus FV 100 confocal microscope (Olympus, Germany) with a 60×- NA:1.35 oil objective. Image analysis and capturing was performed using the Fluoview 2.1c software.

Three-dimensional image analysis. Z-stacks were taken with an interval of 0.1 μm using an Olympus FV 1000 confocal microscope (Olympus, Germany) with 20–30 slices per stack to show cells in their full extension. Stacks were then used for image analysis by IMARIS software (version 7.0.1.1, Bitplane AG, Switzerland), operating with IMARIS Surpass (volume and isosurface rendering analysis) to visualize and locate points of interest (for example, FcγRIIB, dectin-1 and p-Syk expression). For co-localization studies, data sets were analyzed using the IMARIS software.

Surface plasmon resonance analysis. To determine the interactions between FcγRIIB with HiGalH5-ICs and LoGalH5-ICs, surface plasmon resonance was performed using a Biacore 3000 (GE Healthcare) system at 25 °C. FcγRIIB was coupled to the CM5 sensor chip (GE Healthcare) via amine coupling. For activation of the carboxylated dextran matrix of the CM5 chip, 0.05 M *N*-hydroxysuccinimide and 0.2 M *N*-ethyl-*N*-(dimethylamino-propyl) carbodiimide in equal volumes were added to the sensor chip. For immobilization, FcγRIIB was diluted to 34 μg ml^{-1}. Injection of 5 μl receptor resulted in a signal increase of 6,000 resonance units. Unbound reactive groups were saturated with 1 M ethanolamine hydrochloride-NaOH for 7 min. A second flow chamber was subjected to the immobilization protocol but without any addition of protein and served as a reference cell. Serial dilutions of HiGalH5-ICs or LoGalH5-ICs in PBS were added (starting at 10 nM). For detection of binding, the samples were passed over the sensor chip at a constant flow rate of 15 μl min^{-1} for 10 min. BIAevaluation software 3.2 RC1 was used for analysis of the data. First, the binding curves for the different dilutions were overlaid, and the equilibrium

doi:10.1038/nm.2862

response was determined. Then, the equilibrium response of each experiment was used to create saturation curves of analyte binding and to calculate the dissociation constant assuming a 1:1 steady state affinity model.

***In vitro* remodeling of IgG antibodies.** The mouse anti-TNP IgG1 hybridoma antibody (clone H5) was grown for antibody production in RPMI high glucose (GIBCO) supplemented with 0.03% Primatone RL/UF (Sheffield BioScience) and 1% penicillin/streptomycin. Antibodies were purified from cell culture media with protein-G-Sepharose and dialyzed against PBS. *In vitro* galactosylation and/or sialylation was performed in a two-step procedure as described previously[32]. Briefly, 5 mg of antibody were galactosylated by rotating incubation with 75 mU of human β1,4-galactosyltransferase (Calbiochem) and 2 mg of UDP-galactose (Calbiochem) in 1 ml 50 mM MOPS pH 7.2 with 20 mM MnCl2 for 48 h at 37 °C. After buffer exchange to 50 mM MES pH 6.0, IgG was sialylated by incubation with 25 mU of human α2,6-sialyltransferase (Calbiochem) and 0.625 mg of CMP-sialic acid (Calbiochem) for 48 h at 37 °C. H5 IgG1 was degalactosylated by incubation with β-galactosidase (10 mU) from Prozyme (GK80120) for 48 h at 37 °C. IgG antibodies were separated from enzymes by protein G chromatography and dialyzing against PBS. Concentrations of the differentially glycosylated IgG1 antibodies were determined by BCA assays (Pierce) and verified by IgG1 ELISA. Anti-TNP reactivities were measured by ELISA, and N-glycosylation of IgG Fc fragments was characterized by MALDI-TOF mass spectrometry.

Determination of IgG1 glycan composition by MALDI-TOF mass spectrometry. Analysis of N-glycan composition of IgG samples were performed as previously described[39]. Briefly, tryptic glycopeptides obtained from IgG samples were digested with PNGaseF (Sigma-Aldrich), and the resulting N-glycans were purified by C18 and graphitized carbon columns, permethylated according to standard protocols and analyzed by MALDI-TOF mass spectrometry. Spectra were recorded on an Ultraflex III mass spectrometer (Bruker Daltonics) equipped with a Smartbeam laser and a LIFT-MS/MS facility. Calibration was performed on a glucose ladder, and dihydroxybenzoic acid was used as matrix. Spectra were recorded in reflector positive ionization mode, and mass spectra from 3,000 laser shots were accumulated. The data were evaluated using the GlycoWorkbench software and the Glyco-peakfinder tool.

Förster resonance energy transfer. Bone marrow–derived neutrophils were stained with Alexa647-labeled anti–dectin-1 antibody as described above and incubated for 3 min with 1 μg ml^{-1} Cy3-labeled HiGalH5-ICs or LoGalH5-ICs. Subsequently, cells were fixed using diluted Cytofix solution from BD. FRET was measured by determining the fluorescence intensity of the Cy3-HiGalH5-IC or Cy3-LoGalH5-IC donor before and after photobleaching of the Alexa647 anti–dectin-1 antibody acceptor. In FRET, bleaching the acceptor results in an increase in the fluorescent emission of the donor. Cells were imaged with an Olympus FV1000 (Olympus Europa Holding GmbH, Germany) laser scanning microscope, with a 60× 1.40 NA oil objective. Pinhole diameter was set on automatic, and the resolution was set to 320 × 320 pixels at a pixel dwell time of 5 μs. Cy3 was excited at 539 nm, and Alexa647 was excited at 635 nm. An image was acquired once before acceptor bleaching and after photodestruction of the Alexa647 label. For photobleaching, we used the 635-nm laser at 50% of the maximum laser power. The bleaching process was monitored in real time and stopped when 100% of photodestruction was achieved. Then, mean fluorescence intensity of Cy3 and Alexa647 was recorded in different regions of interest on the cell surface using Olympus's FV1000 software (Ver.03.0). The FRET efficiency (E) was calculated as $E = 1 - (I_{DA} / I_D)$, where I_{DA} represents the normalized fluorescence intensity of Cy3 in the presence of nonbleached acceptor. I_D represents the normalized fluorescence intensity of Alexa647 after complete photodestruction of the acceptor.

Statistical analyses. Statistical analysis was performed using the SigmaStat version 3.5 statistical package (Systat Software). With regard to small sample sizes, normal distribution was assumed. To analyze differences between two normally distributed groups, a two-tailed t-test was used. Comparison of the means of more than two normally or non-normally distributed groups was done by one-way analysis of variance (ANOVA) or ANOVA on ranks. When the mean values of the groups showed a significant difference, pairwise comparison was performed using the Tukey test (ANOVA) or Dunn's method (ANOVA on ranks). $P < 0.05$ was considered a significant difference. If not stated otherwise, data were taken from 3–5 individual experiments and expressed as mean values ± s.e.m.

35. Nimmerjahn, F. & Ravetch, J.V. Analyzing antibody-Fc-receptor interactions. *Methods Mol. Biol.* **415**, 151–162 (2008).
36. Graham, I.L., Anderson, D.C., Holers, V.M. & Brown, E.J. Complement receptor 3 (CR3, Mac-1, integrin alpha M beta 2, CD11b/CD18) is required for tyrosine phosphorylation of paxillin in adherent and nonadherent neutrophils. *J. Cell Biol.* **127**, 1139–1147 (1994).
37. Wang, G.G. *et al.* Quantitative production of macrophages or neutrophils ex vivo using conditional Hoxb8. *Nat. Methods* **3**, 287–293 (2006).
38. Rosas, M. *et al.* The induction of inflammation by dectin-1 *in vivo* is dependent on myeloid cell programming and the progression of phagocytosis. *J. Immunol.* **181**, 3549–3557 (2008).
39. Wedepohl, S. *et al.* N-glycan analysis of recombinant L-selectin reveals sulfated GalNAc and GalNAc-GalNAc motifs. *J. Proteome Res.* **9**, 3403–3411 (2010).